Adsorbates in a Box: Titration of Substrate Electronic States

Zhihai Cheng,[1] Jonathan Wyrick,[2] Miaomiao Luo,[1] Dezheng Sun,[2] Daeho Kim,[1] Yeming Zhu,[2] Wenhao Lu,[1] Kwangmoo Kim,[3] T. L. Einstein,[3] and Ludwig Bartels[1,2,*]

[1]*Department of Chemistry, University of California-Riverside, Riverside, California 92521, USA*
[2]*Department of Physics, University of California-Riverside, Riverside, California 92521, USA*
[3]*Department of Physics, University of Maryland, College Park, Maryland 20742-4111, USA*

(Received 24 May 2010; published 6 August 2010)

Nanoscale confinement of adsorbed CO molecules in an anthraquinone network on Cu(111) with a pore size of ≈ 4 nm arranges the CO molecules in a shell structure that coincides with the distribution of substrate confined electronic states. Molecules occupy the states approximately in the sequence of rising electron energy. Despite the sixfold symmetry of the pore boundary itself, the adsorbate distribution adopts the threefold symmetry of the network-substrate system, highlighting the importance of the substrate even for such quasi-free-electron systems.

DOI: 10.1103/PhysRevLett.105.066104 PACS numbers: 68.43.−h, 68.37.Ef, 73.20.−r

Understanding the adsorption of molecular species at solid surfaces resonates as one of the unifying themes throughout the evolution of surface science over the past half-century. The adsorption of an ever-increasing number of molecules on crystallographic surfaces, as well as on steps and at other defect sites, has been studied. Great progress has been made in the development of computational techniques that reveal the electronic interaction between adsorbates and the underlying substrate atoms. However, the effect of lateral confinement of the support on the nanometer scale has remained largely unaddressed because of challenges in the preparation of surfaces covered with atomically identical patterns several nanometers in scale and because of computational limitations in simulating systems consisting of many hundreds of substrate and adsorbate atoms. Yet many of the applications of surface science, for instance in heterogeneous catalysis or in semiconductor processing, crucially rely on nanoscale-delimited surfaces; and recent progress in these fields emphasizes the effects of nanoscale confinement [1] and diminishing scale, respectively.

In this Letter, we address how confinement of the substrate to approximately 4 nm hexagons [2]—i.e., larger than most adsorbate patterns [3–5] and substrate unit cells but smaller than previously investigated structures such as quantum corrals and adislands [6,7]—affects the distribution and energetics of small molecule adsorption. A number of molecular surface networks, including hydrogen bonded [8] and boron-nitride ones [5,9], have been shown to template adsorption of subsequent species [4].

It has been shown that perturbation of substrate electronic states, such as an underlying gas bubble [10] or scattering of a Shockley surface state at a step edge [11] or adatom row [12], affects the distribution of adsorbates. Substrate-mediated long range interactions between molecules have been found in a variety of systems and quantified in a number of cases by scanning tunneling microscopy (STM) [2,13–23] and field ion microscopy [24–26]. A correlation between the location of CO molecules on Ag(111) [27] and benzene on Cu(111) [11], with the phases of the surface scattering amplitude, has been proposed from experimental data and through theoretical modeling [28,29]. In this experimental study we show that confined electronic states of the substrate can actually be titrated with adsorbates, arguably much as electronic states are filled up from the lowest to highest energy in an atomic orbital diagram.

Our measurements were conducted on a Cu(111) surface decorated with a chiral anthraquinone (AQ) network of sixfold symmetry (disregarding the substrate) exhibiting pores that expose 186 substrate atoms in their midst [2] [Fig. 1(a)]. We use CO as our test molecule because a wealth of data on its surface behavior is available: CO molecules adsorb upright atop Cu(111) substrate atoms. They are imaged in STM as protrusions or indentations, depending on whether the STM tip is decorated with a CO atom at its apex or not, respectively [30].

Sample preparation involves the usual sequence of sputtering and annealing, followed by cooling to liquid nitrogen temperatures. The AQ pattern is created by evaporation of the molecule onto the cryogenic sample followed by annealing to room temperature. Deposition of CO molecules through a leak valve onto the AQ-patterned surface at 40 K preserves the pore shapes.

We find that the AQ network blocks the diffusion of adsorbed CO molecules on the substrate; repeated imaging of the same set of pores allows tracking of the perambulation of a fixed number of molecular entities within a confined area. Figures 1(b) and 1(c) show images from a movie [31] of a set of pores, in each of which a few molecules are seen to diffuse. In such sequences of images each molecule can be assigned to a particular substrate atom on which it is adsorbed. From thousands of images obtained, we calculate histograms of the occupation of the

 © 2010 The American Physical Society

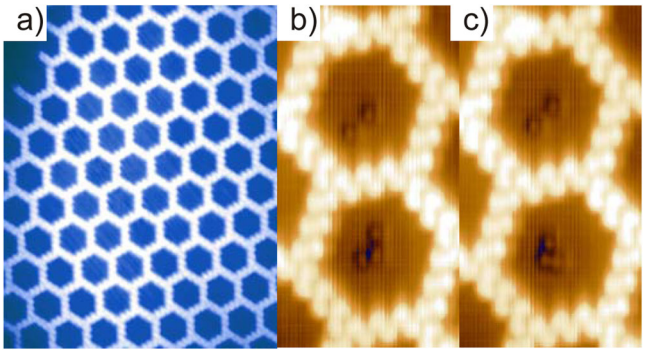

FIG. 1 (color online). (a) An array of atomically defined pores on Cu(111) formed by deposition of anthraquinone according to Ref. [2] Image parameters: 38 nm × 43 nm; Bias: −2.534 V; Current: 50 pA. (b, c) Images from a movie showing the diffusion of two and three CO molecules in confinement. Image parameters: 6 nm × 10 nm; Bias: −2.673 V; Current: 99 pA.

various substrate sites within the confined area [Figs. 2(a)–2(e)]. Each confined area consists of 62 threefold-degenerate (186 in total) adsites surrounding a hollow site at the pore center in a threefold symmetric arrangement. The AQ network is chiral, removing inversion symmetry.

The radial distribution of CO molecules in pores of different coverages is shown in Fig. 3(a). Given the large number of different adsites, we construct seven radial bins, as indicated in the inset of Fig. 3(a). In pores containing a single CO molecule, the CO is generally found at the pore center; in 54% of the cases, the molecule occupies one of the two inner bins of Fig. 3(a). From the distribution of Fig. 2(a), we can obtain the radial variation of the probability P_i of CO occupation of an adsite i indicated in the yellow (front) curve of Fig. 3(a). From this data set we can construct the canonical partition function Z of the single CO system, which allows us to deduce the radial variation of the CO adsorption energy ε [Fig. 3(b)].

$$Z = \sum_i e^{-\varepsilon_i/kT} \quad \text{with} \quad P_i = e^{-\varepsilon_i/kT}/Z$$

with k the Boltzmann constant and T the temperature 27 K of our measurements. The resultant variation of ≈14 meV

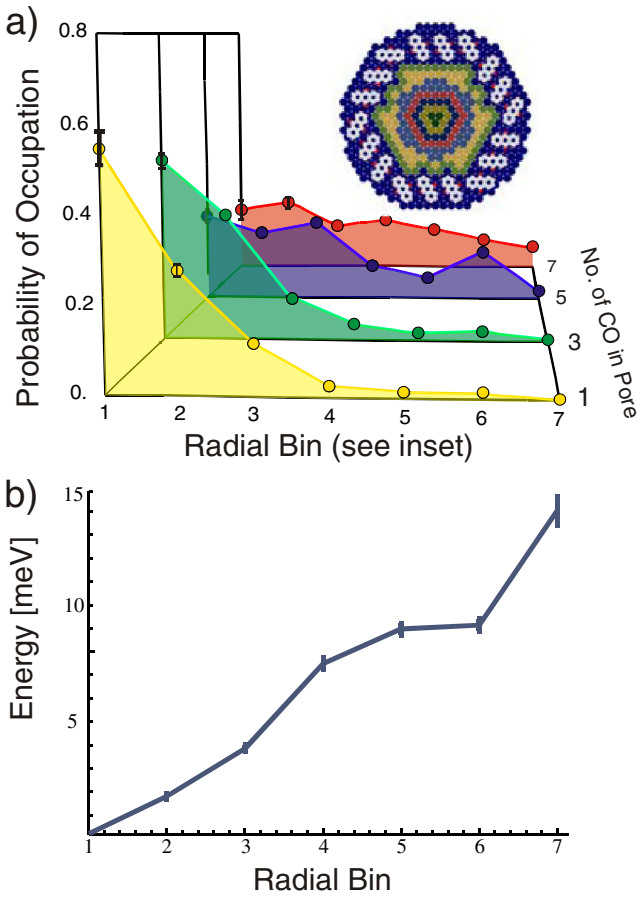

FIG. 3 (color online). (a) Normalized probability of occupation of radial bins (shown in the inset, normalized to the number of substrate sites they encompass) for pores containing 1–7 molecules. For 1,3 molecules, the distribution is monotonic, whereas at increasing number of molecules, an additional intermediate distance also becomes favored until further increase of the coverage renders the plot featureless. (b) Variation of the adsorption energy of a single CO molecule across a pore. Error bars are based on $\sqrt{\text{counts}}$ in the histogram and are shown in panels (a, b) when larger than the data markers.

is quite substantial, approximately 1/5 of the CO/Cu(111) diffusion barrier of 75 meV [16].

For two CO molecules in the system [Fig. 2(b)], we find generally that either both molecules occupy the confinement center or they are split between the center sites and a

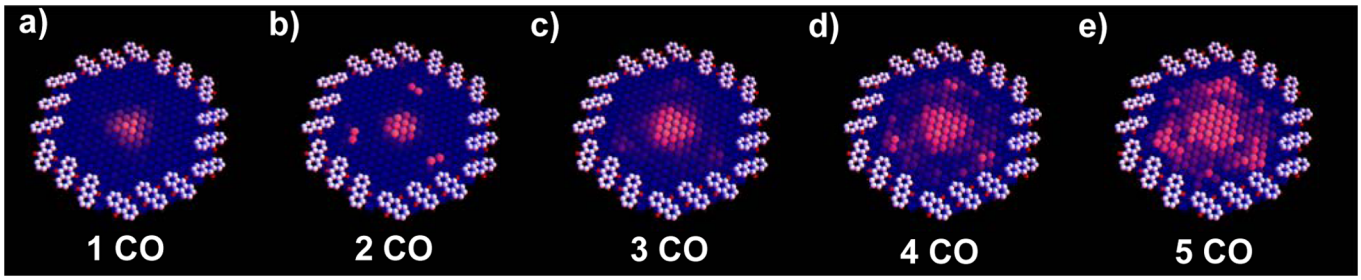

FIG. 2 (color online). Color-coded plots of the probability of CO molecule occupation for each of the 186 Cu substrate atoms exposed within an AQ pore. Each plot is based on >500 CO configurations observed and averaged over equivalent locations.

set of three equivalent adsites approximately halfway towards one set of confinement vertices. The same set of three adsites is also favored in pores that contain 3–5 molecules [Figs. 2(c)–2(e)]. Experimentally, these are independent data sets acquired on different pores, days, and sample preparations; the reappearance of the same location for pores of different coverage rules out experimental error (e.g., through subsurface defects) as the origin of the peripheral peaks in Fig. 2. This poses the question of their physical origin and, in particular, the reason for their threefold symmetry. The ≈ 4 nm diameter of the pore rules out direct intermolecular interactions, suggesting that a substrate-mediated effect may be of relevance. Unfortunately, first-principles computational methods (such as density functional theory) are incapable of treating a system that requires at least 186 substrate atoms per layer (i.e., several hundred in total).

Prompted by the idea that surface states get reconstituted in laterally confined geometries [3,6,32], we turn here to a much simpler continuum model of the surface-bound states derived from the Cu(111) surface state. In this context it is important to realize that although the pore boundary itself is sixfold symmetric, the pore vertices are alternatingly centered on hcp and fcc hollow sites, so that the overall symmetry of the pore on the substrate has the same threefold (and not sixfold) symmetry as the CO distribution [Fig. 2]. Thus, we calculate the confined electronic states within the pore starting from the known solutions of a particle in a triangular box [33], followed by relaxation into the actual geometry of the pore.

Gross *et al.* showed that scattering of the surface state from organic molecules occurs not at the peripheral hydrogen atoms but at the 2nd period elements [34]. Hence, we construct the boundary of our pore from the six carbon and oxygen atoms per molecule (102 in total) that are closest to the pore center. We adapt an iterative finite-difference algorithm [35], more commonly used for solution of Poisson or heat-diffusion equations, to the relaxation of the known solutions into the geometry of the pore. Here, we develop the wave function in a Taylor series to third order; summing over four locations adjacent to a point (x, y) reproduces the Hamiltonian H_{inside} inside the potential-free pore.

$$\frac{\langle x+\delta, y| + \langle x-\delta, y| + \langle x, y+\delta| + \langle x, y-\delta|}{\delta^2}|\varphi\rangle - \frac{4\langle x, y|\varphi\rangle}{\delta^2} \cong \langle x, y|\frac{-2m^*}{\hbar^2}H_{\text{inside}}|\varphi\rangle = \langle x, y|\frac{-2m^*}{\hbar^2}E|\varphi\rangle$$

with m^* the effective mass of an electron of the surface state of 0.34 electron masses and δ a small displacement. Thus, if φ_{n-1} is an approximate eigenfunction of the Hamiltonian, a better approximation φ_n can be found by evaluating

$$\langle x, y|\varphi_n\rangle = \frac{\langle x+\delta, y| + \langle x-\delta, y| + \langle x, y+\delta| + \langle x, y-\delta|}{4 - 2m^*\delta^2 E_{n-1}/\hbar^2}|\varphi_{n-1}\rangle.$$

Alternating this iteration and Gram-Schmidt orthogonalization [36] of the set of eigenfunctions originally obtained from the triangular particle in the box problem, we end up with three eigenfunctions (one unique and one twofold-degenerate) whose eigenvalues E of 170 meV and 440 meV, respectively, are below the Fermi energy E_F, if measured from the bottom of the surface state band of 450 meV below E_F [32,37]. Figures 4(a) and 4(b) show the distribution of local density of state (DOS) associated with the first and twofold-degenerate second state, respectively. Our algorithm provides correct eigenfunctions and eigenstates that are converged and invariant to the grid spacing δ of 1.25 Å, 0.63 Å, or 0.41 Å (corresponding to using a 40×40, 80×80, or 120×120 points grid to represent the pore); however, it cannot guarantee completeness of the set of eigenfunctions and eigenvalues found. Summation of the fraction of the surface Brillouin zone filled by the surface state (characterized by the Fermi vector $k_F = 0.21$ Å^{-1}) [37,38] over the exposed substrate atoms leads to no more than three complete electron pairs in the surface state within each pore, in good agreement with the three states found. This result is further corroborated by the recent finding of Lobo-Checa *et al.* by electron spectroscopy that in a molecular surface network of roughly 1/3 the size of our system, there is exactly one confined state [3].

Comparison between the DOS of Fig. 4 and the molecular distribution within the pore of Fig. 2 shows that CO molecules preferentially occupy locations in the pore that feature a high DOS of the confined surface state, supporting a picture that adsorption energy increases with DOS. Moreover, we find that if only one molecule occupies the

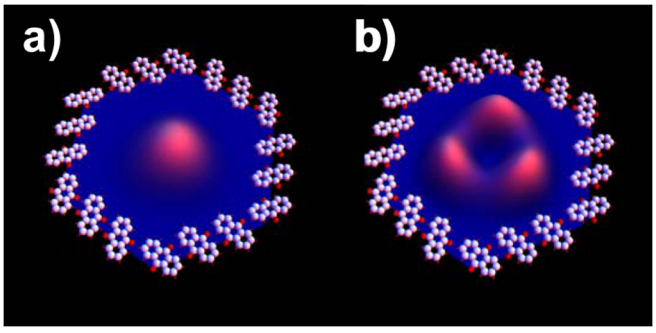

FIG. 4 (color online). Plots of the local DOS of (a) the lowest-energy electronic state of the pore and (b) superposition of the two degenerate second electronic states of the pore. Compare to the distribution of molecules in pores in Fig. 2.

pore, it seeks out preferentially the pore center where the lowest-energy confined surface state is located. Increasing the coverage leads to occupation of locations corresponding to the more energetic second confined state. Thus, increase of the CO coverage may be likened to the ''titration'' of the locations inside the pore that show appreciable local DOS of the confined surface state. The fact that the sequence in which these locations are occupied matches the energetic succession of the corresponding confined surface states reminds one of the filling of electrons into an atomic orbital diagram.

Previous modeling of surface-state-mediated interaction of adsorbates has generally employed a scattering-based formalism related to the modeling of the lateral surface state distribution at E_F visible in STM. This has been shown to work well for systems that involve no confinement of the surface or dimensions much longer than the surface state Fermi wavelength [18,28]. The energy integrated approach described here is more suitable to the relatively small scale of pores in molecular surface networks where the confinement size does not exceed the Fermi wavelength by much. Fiete and Heller showed that for circular quantum corrals at larger corral size, both approaches lead to equivalent results for the energy-resolved surface-state local DOS [32].

Increasing the number of molecules inside the pore beyond the number of electrons in the surface state (i.e., six) causes the radial distribution of molecules in the pore to become more uniform [red curve in Fig. 3(a)], showing the limitation in adsorbate guidance achievable in a pore of given size. This finding corresponds with CO's ability to quench the surface state at relatively low coverage.

Although our calculations were based on free-electron-like behavior of the surface state electrons (i.e., a constant potential within the pore boundary) with just an effective mass accounting for the presence of the substrate, our finding of threefold symmetry (as enforced by the substrate, in contrast to the sixfold symmetry of the molecular network) is crucial for explaining the experimental distribution of adsorbates; this highlights the limitation of the free electron approximation in understanding surface state electrons and their impact on adsorption. In summary, by monitoring adsorbate diffusion within a nanometer-scale confined system we found that such confinement has a pronounced effect on their average location, suggesting that engineering of confinement boundaries may not only allow engineering of surface electronic states but can also be a tool in assembling molecular patterns at surfaces.

We gratefully acknowledge joint NSF Grants No. CHE 07-50334 (T. L. E) and No. 07-49949 (L. B.), as well as the U.S. Department of Energy Grant No. DE-FG02-07ER15842 (L. B.) and secondary support from NSF MRSEC Grant No. DMR 05-20471 and ancillary support from CNAM (T. L. E.).

*Ludwig.Bartels@ucr.edu

[1] M. Haruta, Nature (London) **437**, 1098 (2005).
[2] G. Pawin *et al.*, Science **313**, 961 (2006).
[3] J. Lobo-Checa *et al.*, Science **325**, 300 (2009).
[4] L. Bartels, Nature Chem. **2**, 87 (2010).
[5] M. Corso *et al.*, Science **303**, 217 (2004).
[6] E. Heller *et al.*, Nature (London) **369**, 464 (1994).
[7] M. V. Rastei *et al.*, Phys. Rev. Lett. **99**, 246102 (2007).
[8] J. A. Theobald *et al.*, Nature (London) **424**, 1029 (2003).
[9] S. Berner *et al.*, Angew. Chem., Int. Ed. Engl. **46**, 5115 (2007).
[10] M. Gsell, P. Jakob, and D. Menzel, Science **280**, 717 (1998).
[11] S. J. Stranick, M. M. Kamna, and P. S. Weiss, Science **266**, 99 (1994).
[12] N. N. Negulyaev *et al.*, Phys. Rev. Lett. **101**, 226601 (2008).
[13] E. Sykes *et al.*, Acc. Chem. Res. **36**, 945 (2003).
[14] S. U. Nanayakkara *et al.*, Phys. Rev. Lett. **98**, 206108 (2007).
[15] S. Lukas, G. Witte, and C. Woll, Phys. Rev. Lett. **88**, 028301 (2001).
[16] K. L. Wong *et al.*, J. Chem. Phys. **123**, 201102 (2005).
[17] T. Mitsui *et al.*, Phys. Rev. Lett. **94**, 036101 (2005).
[18] J. Repp *et al.*, Phys. Rev. Lett. **85**, 2981 (2000).
[19] T. L. Einstein, in *Physical Structure of Solid Surfaces, Handbook of Surface Science*, edited by W. N. Unertl (Elsevier, New York, 1996), Vol. 1, p. 577.
[20] K. A. Fichthorn and M. Scheffler, Phys. Rev. Lett. **84**, 5371 (2000).
[21] L. Österlund *et al.*, Phys. Rev. Lett. **83**, 4812 (1999).
[22] V. Stepanyuk *et al.*, Phys. Rev. B **68**, 205410 (2003).
[23] Y. F. Wang *et al.*, J. Am. Chem. Soc. **131**, 10400 (2009).
[24] T. T. Tsong and R. Casanova, Phys. Rev. B **24**, 3063 (1981).
[25] G. L. Kellogg, Surf. Sci. Rep. **21**, 1 (1994).
[26] H. W. Fink and G. Ehrlich, J. Chem. Phys. **81**, 4657 (1984).
[27] M. Kulawik *et al.*, Surf. Sci. **590**, L253 (2005).
[28] P. Hyldgaard and T. L. Einstein, Europhys. Lett. **59**, 265 (2002).
[29] A. Bogicevic *et al.*, Phys. Rev. Lett. **85**, 1910 (2000).
[30] L. Bartels, G. Meyer, and K. Rieder, Appl. Phys. Lett. **71**, 213 (1997).
[31] See supplementary material at http://link.aps.org/supplemental/10.1103/PhysRevLett.105.066104.
[32] G. A. Fiete and E. J. Heller, Rev. Mod. Phys. **75**, 933 (2003).
[33] J. Mathews and R. L. Walker, *Mathematical Methods of Physics* (W. A. Benjamin, New York, 1970).
[34] L. Gross *et al.*, Phys. Rev. Lett. **93**, 056103 (2004).
[35] K. E. Atkinson and W. Han, *Elementary Numerical Analysis* (John Wiley & Sons, New York, 2004).
[36] A. Kiełbasiński and H. Schwetlick, *Numerische Lineare Algebra: Eine Computerorientierte Einführung* (Harri Deutsch, Thun, 1988).
[37] S. D. Kevan and R. H. Gaylord, Phys. Rev. B **36**, 5809 (1987).
[38] L. Burgi *et al.*, Surf. Sci. **447**, L157 (2000).